CBPF-NF-002/81

Fe DIMERS: A THEORETICAL STUDY OF THE HYPERFINE INTERACTIONS

by

Diana Guenzburger and Elisa M. Baggio Saitovitch

Centro Brasileiro de Pesquisas Físicas/CNPq
Av. Wenceslau Braz, 71, fundos - R.J.
Rio de Janeiro - 22290 - Brasil

Fe DIMERS: A THEORETICAL STUDY OF THE HYPERFINE INTERACTIONS

Diana Guenzburger

and

Elisa M. Baggio Saitovitch

Centro Brasileiro de Pesquisas Físicas

Av. Wenceslau Braz, 71 - 22.290 Rio de Janeiro, RJ, Brasil

ABSTRACT

The electronic structures of diatomic molecules Fe_2 and FeM, where M = Mn, Co, Ni and Cu, are investigated by molecular orbitals calculations using a discrete variational method and a local approximation for the exchange interaction. The one-electron wave functions obtained are used to calculate electric field gradients, electronic charge and spin densities at the Fe nucleus and spin-dipolar hyperfine fields, which are related to measured hyperfine parameters reported from experiments in solid inert-gas matrices. Molecular orbitals energies schemes and population analysis are presented. These and other aspects of the electronic structure of the FeM molecules are used in a qualitative interpretation of the hyperfine data; in some cases, are given suggestions for the ground-state configuration.

I INTRODUCTION

Diatomic molecules of transition elements have received considerable attention in recent years, due among other reasons to the interest created by heterogeneous catalysis[1], in which small metal clusters are involved. One experimental technique which makes possible the study of properties of metal dimers is the isolation of such molecules in solid noble gas matrices, where the interaction with the host may be considered negligible for most purposes. In this manner, optical spectra of dimers of first row transition elements were obtained[2], as well as Mössbauer hyperfine parameters of Fe_2[3,4] and mixed Fe dimers[5]. A proper analysis of these measurements requires knowledge of the molecular electronic structures. This presents considerable difficulty, since the degeneracy of the "d" orbitals and small energy difference between 3d and 4s orbitals complicates the application of refined quantum chemistry techniques due to the large number of possible configurations that result, to be included in Configuration-Interaction (C.I.) calculations; this last feature is considered important since correlation effects are expected to be strong even at equilibrium interatomic distances[6,7]. Searching the literature, we have come across non-empirical calculations mainly for Cu_2 and Ni_2, which are more simple to treat than mid-row elements dimers, since the number of "holes" in the "d" band is smaller. However, even for the case of Ni_2 there are discrepancies in the calculations

reported. For example, Xα-scattered wave (XαSW)[8], generalized valence-bond (GVB) with CI[6], "ab initio" with CI[9] or density functional[10] methods were applied to Ni_2, but results lead to no definite conclusion as to the energy ordering of the lowest molecular states.

In this paper, we present the results of a study of the electronic structure of Fe_2 and mixed FeM dimers, where M are different first row transition elements. A somewhat different approach is adopted, as follows: we were interested in understanding and interpreting the hyperfine interactions in these molecules, on which there is a wealth of experimental data (see Table I). At the same time, measurements of these interactions could give information on the electronic structure and chemical bonding. With this in view, we have performed one-determinantal self-consistent field (SCF) calculations for the dimers, using the discreet variational method (DVM)[11] and Xα approximation for the exchange interaction[12]. The molecular orbitals (one-electron functions) obtained were used to calculate quantities related to the hyperfine interactions, i.e., electric field gradients, electron and spin densities at the nucleus, spin-dipole hyperfine fields. Through the relation between these calculated quantities and experimental data, we search for information on the electronic configurations of the dimers. At the same time, the molecular orbital results allow to understand some features relating the hyperfine interactions to characteristics of the chemical bond.

II - DESCRIPTION OF THE CALCULATIONS

II.a - Variational Method

The DVM method[11], originally derived for the calculation of band structures of solids, was later applied to molecules and finite clusters of atoms. We give here a brief summary of its main features. The following error function is defined:

$$f_i(\vec{r}) = (H - E_i)\ \psi_i(\vec{r}) \qquad (1)$$

where ψ_i are one-electron molecular wave functions expanded on a basis of symmetrized atomic orbitals χ_j,

$$\psi_i(\vec{r}) = \sum_j \chi_j(\vec{r}) C_{ji} \qquad (2)$$

A weighted average of $f_i(\vec{r})$ is minimized on a grid of sample points, where the weights are the volume per point, leading to secular equations that allow the determination of the coefficients C_{ji}. We have then, in matrix notation:

$$(\underset{\approx}{H} - \underset{\approx}{E}\ \underset{\approx}{S})\ \underset{\approx}{C} = 0 \qquad (3)$$

These equations are formally identical to the Hartree-Fock-Roothaan equations[13], derived for molecules with the standard Rayleigh-Ritz variational method, except that here the matrix elements of $\underset{\approx}{H}$ and $\underset{\approx}{S}$ are not integrals

but sums over sample points, which greatly simplifies the problem. As the number of points becomes larger, the sums over points approach the integral values. The local exchange potential[12] $V_{X\alpha}$ is employed, defining the molecular Hamiltonian as

$$H = -\frac{1}{2}\nabla^2 + V_{coul} + V_{X\alpha} \qquad (4)$$

where

$$V_{X\alpha}(\vec{r}) = -3\alpha\left[(3/8\pi)\ \rho(\vec{r})\right]^{1/3} \text{ (in Hartrees)} \qquad (5)$$

$\rho(\vec{r})$ being the local electronic density. The basis functions χ_j are symmetrized combinations of numerical atomic orbitals, obtained from Hartree-Fock calculations also with the Xα approximation for the exchange term. The value $\alpha = 2/3$ was used throughout this work.

A model potential is defined for the molecule, to simplify the Coulomb component, expanding the molecular charge in terms of one-center densities[14]:

$$\rho(\vec{r}) \cong \sum_i P_i\ \tilde{\rho}_i(r) \qquad (6)$$

where the subscript i indicates one orbital of a specific atom, and $\tilde{\rho}_i(r)$ is spherically symmetric around each nucleus. P_i are atomic orbital populations, which in the present case are a variation of the standard Mulliken populations, with the overlap population partitioned in a way that the atom with the largest eigenvector coefficient

gets the larger contribution[15]. The populations P_i are iterated to self-consistency. The basis functions used were improved by obtaing self-consistent atomic orbitals for configurations similar to those converged in the molecular calculations. Expansion of the atomic basis was achieved by including diffuse orbitals (4p, 4d, 5s, 5p), kept bound by embedding the atom in a potential well of -2 hartrees and radius $6a_o$. For these simple diatomic molecules of symmetries $D_{\infty h}$ and $C_{\infty v}$, it was possible to reduce the numerical integrations to two dimensions, for which a cylindrical coordinate system was used, with symmetrical grids around each nucleus with points following a logarithmic distribution[16]. This improves the evaluation of the integrals with respect to the statistical Diophantine method[11] used in three dimensions, specially regarding polarized charge distributions; another advantage is the possibility of integrating in only half the z-x plane for $D_{\infty h}$ symmetry (z being the molecular axis), as in Fe_2. The number of integration points needed for a convergence of $\sim$0.001 eV in the eigenvalues was approximatly 3,000, but at least 14,000 were needed in the variational calculation to get meaningful electric field gradient (EFG) matrix elements, due to the large core terms.

II.b - Hyperfine Interactions parameters

Hyperfine parameters may be obtained from calculated molecular wavefunctions. The isomer shift δ, which is a

monopole charge effect caused by the difference in the nuclear radius between excited and ground states in the Mössbauer transition, is given by:

$$\delta = \frac{2}{3} e^2 \pi Z S'_z \left[\langle r^2 \rangle_E - \langle r^2 \rangle_G \right] \left| \rho_A(o) - \rho_S(o) \right| \equiv \beta \Delta \rho(o) \quad (7)$$

where the first brackett represents the difference between the mean square radius of the nucleus in the excited and ground states, and in the second brackett A and S refer to absorber and source. The electronic charge density at the nucleus $\rho(o)$, in the one-electron approximation used, is given by:

$$\rho(o) = \sum_i n_i |\psi_i(o)|^2 \quad (8)$$

where ψ_i is a molecular orbital with occupation n_i. S'_z is a correction factor for relativistic effects, to be used if the wave functions are non-relativistic. The non-spherical charge distribution of the nucleus interacts with a spatially varying electric field caused by the electrons or outer ions in the crystal, originating the quadrupole interaction Δ. The electronic contribution to Δ for linear molecules is:

$$\Delta_e = \frac{1}{2} e^2 Q q \quad (9)$$

where Q is the quadrupole moment of the ^{57}Fe nucleus in the excited state of the 14.4 keV transition (with nuclear spin 3/2), and q is given by a sum of matrix elements over

one-electron functions

$$q = - \sum_i n_i \langle \psi_i(\vec{r}) \left| \frac{3\cos^2\theta - 1}{r^3} \right| \psi_i(\vec{r}) \rangle \qquad (10)$$

where $\vec{r}$ refers to the nucleus of the Mössbauer atom.

Since all the electrons in the diatomic molecules are considered in the present calculations of Δ_e, the only other contribution to Δ is that given by the bare nucleus of the atom other than Fe. We neglect any interactions with the inert gas matrix, since these may be considered weak; furthermore, the atoms of the host do not contribute to Δ as point charges, since they are chargeless.

We have then:

$$\Delta = \Delta_e + \Delta_n = \frac{1}{2} e^2 Q \left[q + Z \left(\frac{3z^2 - r^2}{r^5} \right) \right] \qquad (11)$$

where Z is the atomic number of the other atom and r (or z) the interatomic distance. The Sternheimer core polarization correction factor[17] is not needed since core electrons are included in the molecular orbitals calculation.

The magnetic hyperfine interaction originates from the interaction of the magnetic hyperfine field H_F produced by the electrons of the diatomic molecules and the Fe nucleus seen as a magnetic dipole, and may be divided in three different terms, orbital-dipolar, spin-dipolar and contact[17]. The orbital-dipolar contribution presents the greater difficulties for a calculation and will be neglec-

ted in the present study; one may hope that this is not a too drastic approximation since the orbital angular momentum may be expected to be "quenched" to a certain extent, as compared to the free Fe atom. For totally symmetric (Σ_g or Σ) molecular states, this term is strictly null. The terms considered are then the spin-dipolar field given by:

$$H_D = g\mu_B \sum_j \left\langle \psi_j(\vec{r}) \left| \frac{3\cos^2\theta - 1}{r^3} \right| \psi_j(\vec{r}) \right\rangle \langle s_z^j \rangle \qquad (12)$$

where g is the gyromagnetic ratio, μ_B the Bohr magneton and the sum is over molecular orbitals occupied by unpaired electrons. The contact field is expressed as:

$$H_C = \frac{8\pi}{3} g\mu_B \sum_i \left[|\psi_{i\uparrow}(o)|^2 - |\psi_{i\downarrow}(o)|^2 \right] \times 1/2 \qquad (13)$$

where the molecular orbitals are now obtained in spin-unrestricted calculations, the spatial functions being different for $m_s = +\frac{1}{2}$ and $-\frac{1}{2}$, and is thus proportional to the spin density at the nucleus.

For the calculation of δ and H_C, interpolation of the numerical molecular orbitals to r=0 is straightforward; the calculation of the matrix elements in Eqs. (10) and (12) involves the evaluation of one-center terms, which may be calculated exactly using the eigenvector coefficients and matrix elements between corresponding atomic orbitals, and two-center terms, which require special numerical integration procedures described elsewhere[16][18].

III - SOME ASPECTS OF THE ELECTRONIC STRUCTURE

We shall now discuss some aspects of the molecular orbital picture of the transition elements dimers studied. The molecules considered were Fe_2, FeMn, FeCo, FeNi and FeCu. As mentioned before, the neighbor atoms of the inert gas host were not included in the variational calculation, since they interact weakly with the transition elements. Furthermore, one may expect that any effect of the host will be approximatly the same for all the dimers studied and thus irrelevant when considering trends.

Not much is actually known regarding the local spacial structure of these dimers and their neighbors in the lattice. In an early investigation of Fe_2 [3] isolated in solid noble elements, the Fe atoms were thought to occupy substitutionally two neighbor sites in the host lattice, which was somewhat puzzling since the hyperfine parameters measured were independent of whether the host was solid Ar, Kr or Xe, and these have different lattice parameters. A theoretical study of the Mössbauer hyperfine parameters, employing a semi-empirical molecular orbital method [19] also suggested a large interatomic distance for the dimer. However, very recent measurements [20] using the EXAFS (extended X-ray absorption fine structure) technique have indicated a Fe-Fe distance of 1.87 ± 0.13 Å, shorter than in α-Fe metal or in the molecule in the gaseous state [21]. We have thus considered this as the equilibrium distance in Fe_2 and also in the mixed species FeMn,

FeCo, FeNi and FeCu, for which this information is lacking.

III.a - Fe_2 dimer

The only first principles calculation for Fe_2 was reported by Harris and Jones[10] who employed the density functional method. Following these authors, we may describe roughly the bonding in Fe_2 as resulting from a compromise between different factors. Stabilization is obtained by occupying the lower energy bonding molecular orbitals, rather than those of antibonding nature; this is done, however, at the cost of the exchange interaction stabilization brought in by placing electrons in higher orbitals with spins unpaired. Another factor against a low spin configuration is the fact that in this case the lowest antibonding orbitals of mainly 4s character would be unoccupied, resulting in a s-d charge transfer for the Fe atom in the dimer (with respect to the free atom configuration $3d^6 4s^2$), such configurations being less stable.

The calculations reported by these authors for the lowest energy states suggest that high spin configurations are favoured and the δ_g and δ_u orbitals, of almost pure "3d" character, are only partly filled in Fe_2 and other mid-row elements M_2 dimers, the ground state suggested for $Fe_2(^7\Delta_u)$ pertaining to the configuration; closed shells + $1\delta_g^{\,3} 1\delta_u^{\,2} 3\pi_g^{\,2} 6\sigma_u^{\,1}$.

We have performed self-consistent calculations for six configurations (the six first entries in Table 2),

starting with the configuration given above. The idea was to search for the ground-state configuration, by looking at the calculation (or calculations) that agreed, at least in sign and order of magnitude, with the experimental values of the quadrupole interaction.

In Fig. 1 is shown the behaviour of the one-electron valence energy levels of Fe_2 at different interatomic distances, for configuration $1\delta_g^2 1\delta_u^2 6\sigma_u^2 3\pi_g^2$, a good candidate for the ground state ($^7\Sigma_g$ when all unpaired spins are parallel), as we shall see further on. Only at short energies the "d" orbitals of the two atoms interact, resulting in a splitting of the δ and π levels. The $6\sigma_g$ and $7\sigma_g$ levels have a curious behaviour, caused by the non-crossing rule for levels of the same symmetry: they "repel" each other at $\sim$2 Å, and so exchange 3d and 4s character at short and long distances. Comparison with the atomic 3d and 4s orbital energies, displayed in Fig. 1, also points out to a configuration other than the free atom $3d^6 4s^2$: the assyntotic behaviour of the 3d and 4s levels suggests a configuration nearer $3d^7 4s^1$ for Fe in the dimer. This behaviour at large distances was observed also with the density functional method[10]. The total bond order, which is a measure of the electronic density shared by both atoms, is small (around 0.9), which is consistent with the small dissociation energy of the free molecule Fe_2 (1 eV)[21].

III.b - FeM Molecules

In Table 3 may be seen the populations of the one-

electron valence levels and the total atomic populations for the FeM dimers studied. The mixed dimers show a small charge transfer towards the atom with higher atomic number. The charge transfer increases from FeMn to FeCu. For dimers with mid-row elements, the atomic orbitals of both atoms participate more or less equally in the valence orbitals, but as one goes in the direction of FeCu, there is a tendency to dissociate the valence levels so that those of higher energy have increasing Fe character and those of lower energy otherwise. This is coherent with the valence energy levels schemes of Fig. 2, in which may be seen that the group of higher levels get closer together, in the direction of FeCu. In this latter case, the small splitting of the higher (Fe) levels, together with the smallest bond order of the FeM molecules (0.5) suggests an unbound species, in which case the hypothesis of a small interatomic distance in the solid inert gas matrix may be incorrect.

For all dimers there is a tendency to s-d charge transfer, forming hybrids with configurations different from that of the free atom, in which the 4s orbital is depleted and donates electrons to the 3d (except Cu for which the ground state configuration is $3d^{10}4s^{1}$). The 4p orbital gets a small charge, of the order of 0.1 to 0.3 electrons. Typical atomic configurations from population analysis are given in Table 3. In Table 3 it may also be seen that orbitals of δ symmetries are almost purely "3d"; π orbitals are also of mainly "d" character, those of

higher energy mixing a little of 4p. The σ orbitals have mixed s and d character, with a small p participation in those of higher energy. Only the σ orbitals show significant variations in composition and energy, for different configurations.

IV - HYPERFINE INTERACTIONS

In this section we shall present some results of the calculations of hyperfine interactions parameters and attempt to relate them to the electronic structures.

IV.a - The Quadrupole Interaction

We have tried to reproduce the experimental value of Δ for Fe_2, by performing SCF calculations to obtain q as in Eq. (10). We started with the configuration proposed by Harris and Jones (number (2) in Table 2), which gives a calculated Δ very far from the value measured. Another configuration considered was that proposed by Anderson[27], (number (1) in table), based on a semi-empirical molecular orbital calculation. This gives a large positive value for Δ . In fact, only configurations containing 4 δ electrons give values of the right sign and order of magnitude. The reason for this is made clear when examining Table 4, where the individual valence orbitals contributions are displayed. The δ orbitals, of $3d_{xy(x^2-y^2)}$ character, give large positive one-center contributions to q. All other orbitals give negative one-cen

ter contributions, and it results that configurations δ^4 give the right balance of positive and negative terms. The two-center contributions to q are smaller but mainly negative, and add up to a large negative number. This is cancelled partly by the nuclear contribution $2Z/r^3$ (see Eq. (11)); actually, the core two-center terms are exactly cancelled since they may be considered to be produced by point negative charges on the other nucleus. The contributions of the σ_g orbitals are enhanced by s-d one-center cross terms for q, neglected in atomic models for electric field gradient calculations.

In Table 4 are displayed the individual valence orbitals contributions to q for the FeM molecules. It may be observed that the trend of the one-center contributions from the FeMn to FeCu, i.e., decreasing for the inner valence orbitals and increasing for the outer, is consistent with the trend of the orbital charge distributions shown in Table 3, since the outer valence levels have increasing Fe character. Also in the direction of FeCu there is an increase in the two-center valence contributions, obtained by adding the contributions of individual orbitals if singly occupied (see bottom of columns in Table 4). This may be ascribed to the increasing charge transfer, represented by larger coefficients of the atomic orbitals of element M in Eq. (2), and thus larger contribution of the $-C_M^2 \left\langle \chi_M \left| \frac{3\cos^2\theta - 1}{r^3} \right| \chi_M \right\rangle$ two-center terms to q (M being the element other than Fe).

For Fe_2, the calculated total Δ for configuration

(3) (see Table 2) adds up from the following contributions; one-center, -4.33; two-center, -3.76; nuclear, 2.50 mm/sec. The transformation factor for q given in a.u. is 1 mm/sec = = 2.12 a.u., with Q equal to 0.21 barn in Eq. (11)[17]. In Table 2, besides the six first entries obtained self-consistently, are given results for other configurations, containing 4 δ electrons (we included also configurations with 5 δ electrons when considering the antibonding $7\sigma_u$ orbital occupied), obtained using the molecular orbitals of configuration (3) to calculate q (a "frozen orbitals" scheme). All give large negative values for Δ , although better agreement with the experimental value Δ = -4.05 mm/sec is obtained with configurations (4),(5),(8),(9) and (19). The best agreement seems to be obtained for configuration (4) $1\delta_g^2 1\delta_u^2 6\sigma_u^1 3\pi_g^3$.

A similar study (that is, using this "frozen orbitals" approximation) may be done for the mixed dimers. For FeCu, the smaller number of "holes" restricts the number of possible configurations; in the case of FeCo, one is greatly aided by the measured sign of the field gradient (see Table 1). The configurations that give a semi-quantitative agreement between calculated and measured values of Δ are given in Table 5. In this selection we used information obtained also with the isomer shifts, as shall be seen. For FeMn and FeNi, the large number of holes in the valence orbitals and lack of information on the sign of the field gradient makes the number of possible configurations very high. These results point to a positive

sign for the quadrupole interaction of FeCu. This sign has not yet been measured.

IV.b - The Isomer Shift

The isomer shift depends on the amplitude of the electronic wave function at the origin, according to Eqs. (7) and (8). In a non-relativistic approximation, in linear molecules only orbitals of σ symmetry have non-zero amplitudes at the nucleus.

In Table 6 are displayed the contributions $|\psi_i(o)|^2$ of the molecular orbitals of the dimers to the total electronic density at the Fe nucleus. Only orbitals 7σ to 13σ were considered ($4\sigma_{g(u)}$ to $7\sigma_g$), since our numerical precision is not sufficiently high for the very large core terms; however, *differences* between core electron densities among different Fe ions are known to be very small compared to the outer 3s and 4s contributions[28]. In the dimers, the orbitals 7σ and 8σ ($4\sigma_{g(u)}$ for Fe_2) represent almost totally the contribution of the 3s orbital of Fe, and the higher orbitals that of the 4s.

It is seen in the table that the sum of these orbitals contributions to ρ(o), if occupied by the same number of electrons, is very similar. A small decrease in ρ(o) from FeMn to FeCu is observed. This may be related to the trend in the 3d and 4s populations of the dimers shown in Table 3. If one uses an atomic model for this problem, ρ(o) increases with increasing Fe 4s population

and decreasing 3d (since 3d electrons "shield" the 3s and 4s). Accordingly, Table 3 shows increasing 3d and decreasing 4s populations on Fe from FeMn to FeCu. Orbital distortions are also important, but may be expected to cancel approximately when observing this trend among the dimers, if these molecules have approximately the same interatomic distance, as implied in these calculations.

It is curious to notice that this same trend in $\rho(o)$ for the dimers explains qualitatively the observed isomer shifts of Fe impurities in transition metals Mn to Cu, as well as the isomer shifts of first-neighbour Fe atoms in Fe metal containing Mn, Co, Ni and Cu impurities[29]. In fact, in these cases there is a tendency towards larger isomer shifts for Fe from Mn to Cu, either as hosts or impurities. This corresponds to a *decrease* in $\rho(o)$, since $[\langle r^2\rangle_E - \langle r^2\rangle_G]$ in Eq. (7) is negative for the 14.4 keV transition of ^{57}Fe. This suggests that isomer shifts of systems involving transition elements metallic bonds depend on fundamental features that may be represented by a single bond between two atoms. In the present case of diatomic molecules, the charge transfer to the atom other than Fe depletes mainly the outer σ orbitals, since they are much involved in bonding, resulting in smaller 4s populations on Fe: the increase in the 3d populations could be ascribed to a synergic effect destined to maintain charge neutrality.

In the case of Fe_2, we have also investigated the effect of different interatomic distances on $\rho(o)$, for a given configuration. The results are shown in Fig. 3. There

is a drammatic increase of $\rho(o)$ at shorter distances, not followed by any significant changes of 4s or 3d populations, and which may be interpreted as an orthogonality effect ("overlap distortion") roughly described as follows: at shorter distances, the valence electrons on one atom tend to contract, to avoid the electrons on the core molecular orbitals of the other atom. Again, this trend may be related to the trend observed for isomer shifts of Fe metal at different pressures[29]: at higher pressures, the isomer shifts are smaller. In the present case of this molecular orbital picture of Fe dimers, orbital contractions are expressed by greater participation (although still to a small extent) of inner atomic orbitals (mainly 3s) in the valence σ molecular orbitals, according to Eq. (2).

Is there any observable trend for the isomer shifts of Fe in the Fe dimers considered, as in the case of impurities in metals? Observing Table 1, it is clear that there is not. The conclusion is that the different dimers must have a different number of σ electrons. To try to gain some insight into this problem, we plotted in Fig.4 the isomer shifts δ given in Table 1 for Fe ions or atoms isolated in inert matrices against values of $\rho(o)$ (3s+4s) and drawed, on the same figure, lines representing the values of δ for Fe dimers. It may be expected that $\rho(o)$ for these dimers will fall near the line that links the points pertaining to $Fe^{+1}(3d^7)$, $Fe^{+1}(3d^6 4s^1)$ and Fe $(3d^6 4s^2)$; $\rho(o)$ for these were obtained with Hartree-Fock calculations in the Xα approximation, for the same va-

lue of $\alpha(=2/3)$. Examining this figure and Table 1, it is clear that FeCo and FeCu have the smaller number of σ electrons, FeMn and Fe_2 an intermediate number and FeNi a larger number. These considerations were taken into account when constructing the "frozen orbitals" configurations of Table 5 for FeCo and FeCu: we have made the hypothesis of two 12σ - 13σ electrons for FeCo and two or three for FeCu. For Fe_2, configurations resulting in a value of $\rho(o)$ around 148 a_o^{-3} should be favoured; however, this parameter is not so sensitive as Δ, since, as seen in Table 2, almost all configurations considered give "acceptable" values of $\rho(o)$, making allowances for computational errors.

IV.c - Magnetic hyperfine interactions

To investigate some of the effects of unpaired spins, we have performed spin-unrestricted self-consistent calculations for Fe_2 at 1.87 Å interatomic distance, for two configurations, namely $1\delta_{g\uparrow}^2 1\delta_{u\uparrow}^2 6\sigma_{u\uparrow}^1 3\pi_{g\uparrow}^2 7\sigma_{u\uparrow}^1 ({}^9\Sigma_g)$ and $1\delta_{g\uparrow}^2 1\delta_{g\downarrow}^1 1\delta_{u\uparrow}^2 6\sigma_{u\uparrow}^1 3\pi_{g\uparrow}^2 ({}^7\Delta_u)$. The energies of the molecular orbitals are given in Figs. 5 and 6. It may be observed that the orbitals with $\langle S_z \rangle = 1/2$ have considerably lower energies than the corresponding orbitals with $\langle S_z \rangle = -1/2$. The spin density along the z axis is drawn in Fig. 7 for configuration $1\delta_{g\uparrow}^2 1\delta_{u\uparrow}^2 6\sigma_{u\uparrow}^1 3\pi_{g\uparrow}^2 7\sigma_{u\uparrow}^1 ({}^9\Sigma_g)$; the assymetry with respect to the Fe nucleus is evident, the spin density being more extended between the atoms. For ${}^7\Delta_u$, this effect is weaker. In Table 7 the spin densities at the Fe

nucleus for individual orbitals are given. It is noticeable that the core polarization obtained, especially regarding the 2s contribution to $[\rho_{\uparrow}(o) - \rho_{\downarrow}(o)]$ which corresponds to the pair $(2\sigma_g, 2\sigma_u)$ in Fe_2, is quite small when compared to the Fe atom $(3d^6 4s^2)$, also calculated in the Xα approximation. This could be due to the spin-density asymmetry mentioned. The valence electrons in $6\sigma_g$ give a negative contribution, in contrast with the polarization effect of 4s electrons in the atom.

Going back to Table 2, we show the values of the hyperfine field, including contact and spin-dipolar contributions, for Fe_2, calculated according to Eqs. (12) and (13). For configurations marked (+), self-consistent field calculations were performed. For the others, the "frozen-orbitals" procedure already described was adopted using the spin-polarized orbitals of configuration number (2). The information conveyed as to which should be the ground state configuration is small, especially since the sign of the hyperfine field was not measured. Again, configuration number (4) gives $|H_F|$ that compares reasonably well with experiment. In general, configurations that give small calculated absolute values of the hyperfine field are less likely, since the measured field is high (see Table 1). It should be mentioned that the Xα exchange approximation underestimates the spin polarization of the core electrons[12].

V - CONCLUSION

In spite of its apparent simplicity, the problem of describing the electronic structure of diatomic molecules of transition elements is a complex one, due to the participation of the degenerate d orbitals which are near in energy to the 4s. This generates a large number of nearly-degenerate molecular orbitals, and thus many possible configurations of similar energies. The problem of determining the ground state and configuration is thus not a trivial one.

Here we have adopted a simple approach, the DVM method, to calculate molecular orbitals of FeM dimers (M=Mn, Fe, Co, Ni and Cu). The calculations include all electrons and are iterated to self-consistent populations; however, no Configuration-Interaction was done (although the Xα approximation for the exchange interaction is claimed to take into account part of electron correlation[12]) and the treatment of open shells is only approximate. Nevertheless, we believe that this study has given insight into some general features of bonding in the FeM molecules, and helped understand the hyperfine interactions measured by Mössbauer spectroscopy.

Acknowledgements

The authors are grateful to D.E.Ellis for interesting discussions and to G.K.Shenoy for information on the Fe_2 interatomic distance prior to publication.

REFERENCES

1. J.H.Sinfelt, Science, 195, 641 (1977).
2. M.Moskovits and J.E.Hulse, J.Chem. Phys., 66, 3988 (1977); T.C.DeVore, A.Ewing, H.F.Fransen and V.Calder, Chem.Phys. Letters, 35, 78 (1975).
3. T.K.McNab, H.Micklitz and P.H.Barrett, Phys. Rev., B4, 3787 (1971).
4. P.A.Montano, P.H.Barrett and Z.Shanfield, J.Chem. Phys., 64, 2896 (1976).
5. W.Dyson and P.A.Montano, Phys. Rev. B20, 3619 (1979); W.Dyson and P.A.Montano, Solid State Comm., 33, 191 (1980).
6. T.H.Upton and W.A.Goddard III, J.Am.Chem.Soc., 100, 5659 (1978).
7. M.F.Guest, I.H.Hillier and C.D.Garner, Chem. Phys. Letters, 48, 587 (1977).
8. N.Rösch and T.N.Rhodin, Phys. Rev. Lett., 32, 1189 (1974).
9. I.Shim, J.P.Dahl and H.Johansen, Int. J.Quant. Chem., 15, 311 (1979).
10. J.Harris and R.O.Jones, J.Chem. Phys. 70, 830 (1979).
11. D.E.Ellis and G.S.Painter, Phys. Rev. B2, 2887 (1970); D.E.Ellis, Int. J. Quant. Chem., 52, 35 (1968).
12. J.C.Slater, "Quantum Theory of Molecules and Solids", Vol. IV, MacGraw-Hill, New York (1974).
13. C.C.J.Roothaan, Rev. Mod. Phys., 23, 69 (1951).
14. A.Rosén, D.E.Ellis, H.Adachi and F.W.Averill, J.Chem.Phys., 85, 3629 (1976).
15. C.Umrigar and D.E.Ellis, Phys. Rev., B21, 852 (1980).
16. Diana Guenzburger and D.E.Ellis, Phys. Rev. B, in press.

17. N.N.Greenwood and T.C.Gibb, "Mössbauer Spectroscopy", Chapman and Hall, London (1971).

18. H.B.Jansen and D.E.Ellis, to be published.

19. A.Trautwein and F.E.Harris, Phys. Rev., B7, 4755 (1973).

20. P.A.Montano and G.K.Shenoy, to be published.

21. S.S.-Lin and A.Kant, J.Phys. Chem., 73, 2450 (1969).

22. H.Micklitz and F.J.Litterst, Phys. Rev. Letters, 33, 480 (1974).

23. P.A.Montano, P.H.Barrett, H.Micklitz, A.J.Freeman and J.V.Mallow, Phys. Rev., B17, 6 (1978).

24. H.Micklitz and P.H.Barrett, Phys. Rev. Letters, 28, 1547 (1972).

25. W.Dyson and P.A.Montano, J. Am. Chem. Soc., 100, 7439 (1978).

26. P.A.Montano, J. Appl. Physics, 49, 1561 (1978).

27. A.B.Anderson, Phys. Rev., B16, 900 (1977).

28. J.V.Mallov, A.J.Freeman and J.P.Desclaux, Phys. Rev., B13, 1884 (1976).

29. R.Ingalls, F.van der Woude and G.A.Sawatzky, in"Mössbauer Isomer Shifts", ed. G.K.Shenoy and F.E.Wagner, North-Holland, Amsterdam (1978), ch. 7.

TABLE CAPTIONS

Table 1 Experimental hyperfine data for Fe atom, ions and dimers isolated in solid rare-gas matrices. Values of δ are relative to Fe metal.

a) From Ref. (3).

b) From Ref. (4).

c) From Ref. (22).

d) From Ref. (23).

e) From Ref. (24).

f) From Ref. (5).

g) From Ref. (25).

h) From Ref. (26).

Table 2 Calculated hyperfine parameters for Fe_2.

Table 3 Populations of molecular orbitals (in % of one electron), atomic orbitals populations and charges for Fe dimers. Only molecular orbital populations > 5% are mentioned. Atomic orbitals 4d, 5s and 5p, present in the basis, show very small populations in the molecule.

Table 4 One-center and two-center contributions to the matrix elements $-\langle\psi_i\left|\frac{3\cos^2\theta-1}{3}\right|\psi_i\rangle$ for molecular orbitals of Fe dimers. Two-center contributions are given in paranthesis. In atomic units (1 mm/sec= 2.12 a.u.).

Table 5 Calculated values of Δ and $\rho(o)$ for FeCo and FeCu. Configurations marked (*) were converged to self-consistency, and the orbitals obtained were used to calculate Δ for the other configurations.

Table 6 Values of the electronic density at the Fe nucleus $|\psi_i(o)|^2$ for valence molecular orbitals of Fe dimers (in a_o^{-3}).

Table 7 Values of the spin densities at an Fe nucleus for Fe_2 and Fe (in a_o^{-3}).

FIGURE CAPTIONS

Figure 1 Orbital energies for Fe_2, and for Fe in different configurations. Configuration $3d^{6.5}4s^{1.1}4p^{0.3}$ corresponds approximately to that of the Fe atom in the dimer, obtained by population analysis.

Figure 2 Orbital energies for Fe dimers, with configurations corresponding to high spin states. Unmarked orbitals are doubly occupied (except $7\sigma_u$ and 14σ).

Figure 3 Values of $\rho(o)$ (core orbitals 1σ to 3σ excluded) at an Fe nucleus of Fe_2, at different interatomic distances, for configuration $(...1\delta_g^{\,2}1\delta_u^{\,2}6\sigma_u^{\,2}3\pi_g^{\,2})$.

Figure 4 Experimental values of δ, relative to Fe metal (see Table 1), plotted against electronic densities at the Fe nucleus for Fe atoms, ions and dimers (only 3s and 4s contributions).

Figure 5 Orbital energies of Fe_2 in a spin-polarized calculation for configuration $(1\delta_{g\uparrow}^{\,2}1\delta_{u\uparrow}^{\,2}6\sigma_{u\uparrow}^{\,1}3\pi_{g\uparrow}^{\,2}7\sigma_{u\uparrow}^{\,1})$ and orbital energies of Fe atom.

Figure 6 Orbital energies of Fe_2 in a spin-polarized calculation for configuration $(1\delta_{g\uparrow}^{\,2}1\delta_{g\downarrow}^{\,1}1\delta_{u\uparrow}^{\,2}6\sigma_{u\uparrow}^{\,1}3\pi_{g\uparrow}^{\,2})$.

Figure 7 Total spin density $\sum_i \left[\, |\psi_{i\uparrow}(\vec{r})|^2 - |\psi_{i\downarrow}(\vec{r})|^2 \,\right]$ along the molecular axis z for Fe_2 in configuration $(1\delta_{g\uparrow}^{\,2}1\delta_{u\uparrow}^{\,2}6\sigma_{u\uparrow}^{\,1}3\pi_{g\uparrow}^{\,2}7\sigma_{u\uparrow}^{\,1})$, the origin being the midpoint between the atoms.

TABLE 1

Fe species	δ (mm/sec)	Δ (mm/sec)	H_F (k0e)
$Fe(3d^6 4s^2)$	-0.75 ± 0.03 [a]	-	$\lvert 800 \rvert \pm 15$ [b]
$Fe^{+1}(3d^6 4s^1)$	$+0.26 \pm 0.03$ [c]	-	$H_z = 350$ $H_x = H_y = 700$ [d]
$Fe^{+1}(3d^7)$	$+1.77 \pm 0.02$ [e]	-	
Fe_2	-0.14 ± 0.02 [a]	-4.05 ± 0.04 [a] [f]	$\lvert 600 \rvert \pm 15$ [b]
FeMn	0.24 ± 0.03 [g]	$\lvert 1.93 \rvert \pm 0.03$ [g]	
FeCo	0.55 ± 0.05 [h]	-3.60 ± 0.05 [h]	
FeNi	-0.54 ± 0.05 [h]	$\lvert 1.95 \rvert \pm 0.05$ [h]	
FeCu	0.46 ± 0.07 [h]	$\lvert 1.63 \rvert \pm 0.07$ [h]	

TABLE 2

CONFIGURATION (closed shells + ...)	Δ (mm/sec)	$\rho(o)$ (a_o^{-3})	$H_F(H_C + H_D)$ (k0e)
1. * $7\sigma_g^1 1\delta_g^4 1\delta_u^2 6\sigma_u^1 3\pi_g^2$	+4.2	148.30	+690
2. * $7\sigma_g^2 1\delta_g^3 1\delta_u^2 6\sigma_u^1 3\pi_g^2$	-0.51	148.82	+583$^+$
3. * $7\sigma_g^2 1\delta_g^2 1\delta_u^2 6\sigma_u^2 3\pi_g^2$	-5.6	149.68	-210
4. * $7\sigma_g^2 1\delta_g^2 1\delta_u^2 6\sigma_u^1 3\pi_g^3$	-4.6	148.81	+470
5. * $7\sigma_g^2 1\delta_g^2 1\delta_u^2 3\pi_g^4$	-3.0	149.07	-161
6. * $1\delta_g^2 7\sigma_g^2 1\delta_u^2 3\pi_g^2 6\sigma_u^1 7\sigma_u^1$	-6.4	149.36	+849$^+$
7. $7\sigma_g^2 1\delta_g^2 1\delta_u^2 6\sigma_u^2 3\pi_g^4$	-5.3	147.45	-1205
8. $7\sigma_g^1 1\delta_g^2 1\delta_u^2 6\sigma_u^2 3\pi_g^3$	-5.0	148.76	-220
9. $7\sigma_g^1 1\delta_g^2 1\delta_u^2 6\sigma_u^1 3\pi_g^4$	-4.9	147.50	+457
10. $7\sigma_g^2 1\delta_g^2 1\delta_u^2 6\sigma_u^2 3\pi_g^1 7\sigma_u^1$	-5.6	150.29	+71
11. $7\sigma_g^2 1\delta_g^2 1\delta_u^2 6\sigma_u^1 3\pi_g^1 7\sigma_u^2$	-6.6	149.25	+650
12. $7\sigma_g^2 1\delta_g^3 1\delta_u^2 6\sigma_u^1 3\pi_g^1 7\sigma_u^1$	-1.6	149.03	+865
13. $7\sigma_g^1 1\delta_g^2 1\delta_u^2 6\sigma_u^2 3\pi_g^2 7\sigma_u^1$	-6.0	148.98	+140
14. $7\sigma_g^1 1\delta_g^2 1\delta_u^2 6\sigma_u^1 3\pi_g^3 7\sigma_u^1$	-5.9	147.72	+818
15. $7\sigma_g^1 1\delta_g^2 1\delta_u^2 6\sigma_u^1 3\pi_g^2 7\sigma_u^2$	-6.9	147.94	+719
16. $7\sigma_g^1 1\delta_g^2 1\delta_u^2 6\sigma_u^2 3\pi_g^1 7\sigma_u^2$	-7.0	149.20	-36
17. $7\sigma_g^1 1\delta_g^3 1\delta_u^2 6\sigma_u^2 3\pi_g^1 7\sigma_u^1$	-2.0	148.98	+178
18. $7\sigma_g^1 1\delta_g^3 1\delta_u^2 6\sigma_u^1 3\pi_g^2 7\sigma_u^1$	-2.0	147.72	+934
19. $7\sigma_g^1 1\delta_g^3 1\delta_u^2 6\sigma_u^1 3\pi_g^1 7\sigma_u^2$	-3.0	147.94	+757

TABLE 3

Orbital	FeMn ($1\delta^2 2\delta^2 1\sigma^2 6\pi^1$)	Fe_2 ($1\delta_g^2 1\delta_u^2 6\sigma_u^2 3\pi_g^2$)		FeCo ($1\delta^3 2\delta^2 1\sigma^2 6\pi^2$)	FeNi ($1\delta^4 2\delta^2 1\sigma^2 6\pi^2$)	FeCu ($1\delta^4 1\sigma^2 2\delta^3 6\pi^2$)
11σ	9(4s), 50(3d)-Fe 34(3d)-Mn	$6\sigma_g$	22(4s) 73(3d)	8(4s),31(3d)-Fe 16(4s),39(3d)-Co	7(4s),28(3d)-Fe 21(4s),37(3d)-Ni	16(3d)-Fe 9(4s),69(3d)-Cu
5π	61(3d)-Fe 37(3d)-Mn	$3\pi_u$	97(3d)	40(3d)-Fe 58(3d)-Co	36(3d)-Fe 61(3d)-Ni	12(3d)-Fe 87(3d)-Cu
12σ	43(4s), 12(3d)-Fe 39(4s)-Mn	$7\sigma_g$	72(4s) 27(3d)	33(4s),11(3d)-Fe 36(4s),19(3d)-Co	32(4s),10(3d)-Fe 32(4s),25(3d)-Ni	22(4s)-Fe 59(4s),16(3d)-Cu
1δ	83(3d)-Fe 16(3d)-Mn	$1\delta_g$	100(3d)	23(3d)-Fe 77(3d)-Co	15(3d)-Fe 84(3d)-Ni	99(3d)-Cu
2δ	19(3d)-Fe 81(3d)-Mn	$1\delta_u$	100(3d)	75(3d)-Fe 24(3d)-Co	83(3d)-Fe 17(3d)-Ni	97(3d)-Fe
13σ	13(4s), 26(3d)-Fe 16(4s), 40(3d)-Mn	$6\sigma_u$	24(4s) 68(3d)	11(4s),42(3d)-Fe 10(4s),31(3d)-Co	11(4s),4s(3d)-Fe 8(4s),29(3d)-Ni	14(4s),62(3d)-Fe 7(4s),12(3d)-Cu
6π	39(3d)-Fe 57(3d)-Mn	$3\pi_g$	97(3d)	56(3d)-Fe 42(3d)-Co	58(3d)-Fe 39(3d)-Ni	78(3d)-Fe 5(4p),16(3d)-Cu
Atomic Configuration	Fe($3d^{6.57}4s^{1.26}4p^{0.16}$) Mn($3d^{5.67}4s^{1.19}4p^{0.10}$)	$3d^{6.61}4s^{1.21}4p^{0.12}$		Fe($3d^{6.66}4s^{1.14}4p^{0.09}$) Co($3d^{7.65}4s^{1.24}4p^{0.14}$)	Fe($3d^{6.67}4s^{1.13}4p^{0.07}$) Ni($3d^{8.67}4s^{1.23}4p^{0.15}$)	Fe($3d^{6.75}4s^{0.94}4p^{0.05}$) Cu($3d^{9.61}4s^{1.37}4p^{0.20}$)
Charges	Fe -0.02 Mn +0.02	-		Fe +0.07 Co -0.07	Fe +0.10 Ni -0.10	Fe +0.22 Cu -0.22

TABLE 4

	FeMn $(1\delta^2 2\delta^2 13\sigma^2 6\pi^1)$	Fe_2 $(1\delta_g^2 1\delta_u^2 6\sigma_u^2 3\pi_g^2)$		FeCo $(1\delta^3 2\delta^2 13\sigma^2 6\pi^2)$	FeNi $(1\delta^4 2\delta^2 13\sigma^2 6\pi^2)$	FeCu $(1\delta^4 13\sigma^2 2\delta^3 6\pi^2)$
11σ	-1.193 (-0.508)	$6\sigma_g$	-0.859 (-0.538)	-0.701 (-0.559)	-0.631 (-0.555)	-0.434 (-0.429)
5π	-0.654 (-0.024)	$3\pi_u$	-0.498 (-0.028)	-0.399 (-0.032)	-0.367 (-0.034)	-0.094 (-0.043)
12σ	-0.472 (0.150)	$7\sigma_g$	-0.461 (0.109)	-0.382 (0.083)	-0.348 (0.055)	-0.094 (0.003)
1δ	2.135 (-0.004)	$1\delta_g$	1.252 (-0.015)	0.569 (-0.026)	0.383 (-0.029)	0.031 (-0.037)
2δ	0.532 (-0.030)	$1\delta_u$	1.389 (-0.020)	2.056 (-0.011)	2.237 (-0.008)	2.547 (-0.001)
13σ	-0.725 (0.053)	$6\sigma_u$	-0.922 (0.053)	-1.078 (0.007)	-1.142 (-0.011)	-1.391 (-0.208)
6π	-0.467 (-0.015)	$3\pi_g$	-0.636 (-0.013)	-0.744 (-0.012)	-0.783 (-0.011)	-1.032 (-0.004)
$-\sum_i \langle\psi_i\left\|\frac{3\cos^2\theta-1}{r^3}\right\|\psi_i\rangle$	0.702 (-0.451)	0.772 (-0.526)		0.803 (-0.631)	0.819 (-0.675)	0.985 (-0.804)

TABLE 5

Dimer	Configuration (closed shells + ...)	Δ (mm/sec)	ρ(o) (a_o^{-3})
FeCo	(1) $12\sigma^2 1\delta^3 2\delta^2 13\sigma^2 6\pi^2$ (*)	-4.11	149.29
	(2) $12\sigma^1 1\delta^3 2\delta^2 13\sigma^1 6\pi^4$	-4.40	146.84
	(3) $12\sigma^2 1\delta^3 2\delta^2 6\pi^4$	-2.77	147.41
FeCu	(1) $1\delta^4 12\sigma^2 13\sigma^2 2\delta^3 6\pi^2$ (*)	+1.78	148.57
	(2) $1\delta^4 12\sigma^1 13\sigma^1 2\delta^3 6\pi^4$	+0.97	145.77
	(3) $1\delta^4 12\sigma^2 13\sigma^1 2\delta^3 6\pi^3$	+2.97	147.69
	(4) $1\delta^4 12\sigma^1 13\sigma^1 2\delta^3 6\pi^3 14\sigma^1$	+1.10	146.45

TABLE 6

	FeMn $(1\delta^2 2\delta^2 13\sigma^2 6\pi^1)$	Fe_2 $(1\delta_g^2 1\delta_u^2 6\sigma_u^2 3\pi_g^2)$		FeCo $(1\delta^3 2\delta^2 13\sigma^2 6\pi^2)$	FeNi $(1\delta^4 2\delta^2 13\sigma^2 6\pi^2)$	FeCu $(1\delta^4 13\sigma^2 2\delta^3 6\pi^2)$
7σ	70.34	$4\sigma_g$	34.92	0.03	0.01	0.
8σ	0.10	$4\sigma_u$	35.49	70.37	70.40	70.35
9σ	0.07	$5\sigma_g$	0.09	0.05	0.04	0.05
10σ	0.03	$5\sigma_u$	0.	0.02	0.02	0.02
11σ	1.15	$6\sigma_g$	1.61	1.72	1.80	1.06
12σ	2.36	$7\sigma_g$	1.69	1.51	1.31	1.92
13σ	1.01	$6\sigma_u$	1.04	0.94	0.93	0.88
$\sum_i \lvert\psi_i(o)\rvert^2$	75.05		74.84	74.65	74.51	74.28
$2\sum_i \lvert\psi_i(o)\rvert^2$	150.10		149.68	149.29	149.02	148.57

TABLE 7

Fe_2 $\left(1\delta_{g\uparrow}^2\ 1\delta_{u\uparrow}^2\ 6\sigma_{u\uparrow}^1\ 3\pi_{g\uparrow}^2\ 7\sigma_{u\uparrow}^1\right)$			Fe $(3d_\uparrow^5 3d_\downarrow^1 4s_\uparrow^1 4s_\downarrow^1)$		Fe $(3d_\uparrow^5\ 3d_\downarrow^2 4s_\uparrow^1)$	
orbital	$[\psi_{i\uparrow}(o)\|^2-\|\psi_{i\downarrow}(o)\|^2]$		orbital	$\|y_o^o\|^2[R_\uparrow^2(o)-R_\downarrow^2(o)]$	orbital	$\|y_o^o\|^2[R_\uparrow^2(o)-R_\downarrow^2(o)]$
$1\sigma_g$	-0.019	-0.037	1s	-0.052	1s	-0.011
$1\sigma_u$	-0.018					
$2\sigma_g$	-0.198	-0.390	2s	-1.689	2s	-1.126
$2\sigma_u$	-0.192					
$3\sigma_g$	0.0	0.0	3s	0.756	3s	0.419
$3\sigma_u$	0.0					
$4\sigma_g$	0.253	0.486	4s	1.176	4s	3.932
$4\sigma_u$	0.233					
$5\sigma_g$	0.	0.				
$5\sigma_u$	0.					
$6\sigma_{g\uparrow\downarrow}^2$	-0.483	-0.176				
$6\sigma_{u\uparrow}^1$	0.307					
$7\sigma_{g\uparrow\downarrow}^2$	0.710	1.965				
$7\sigma_{u\uparrow}^1$	1.255					

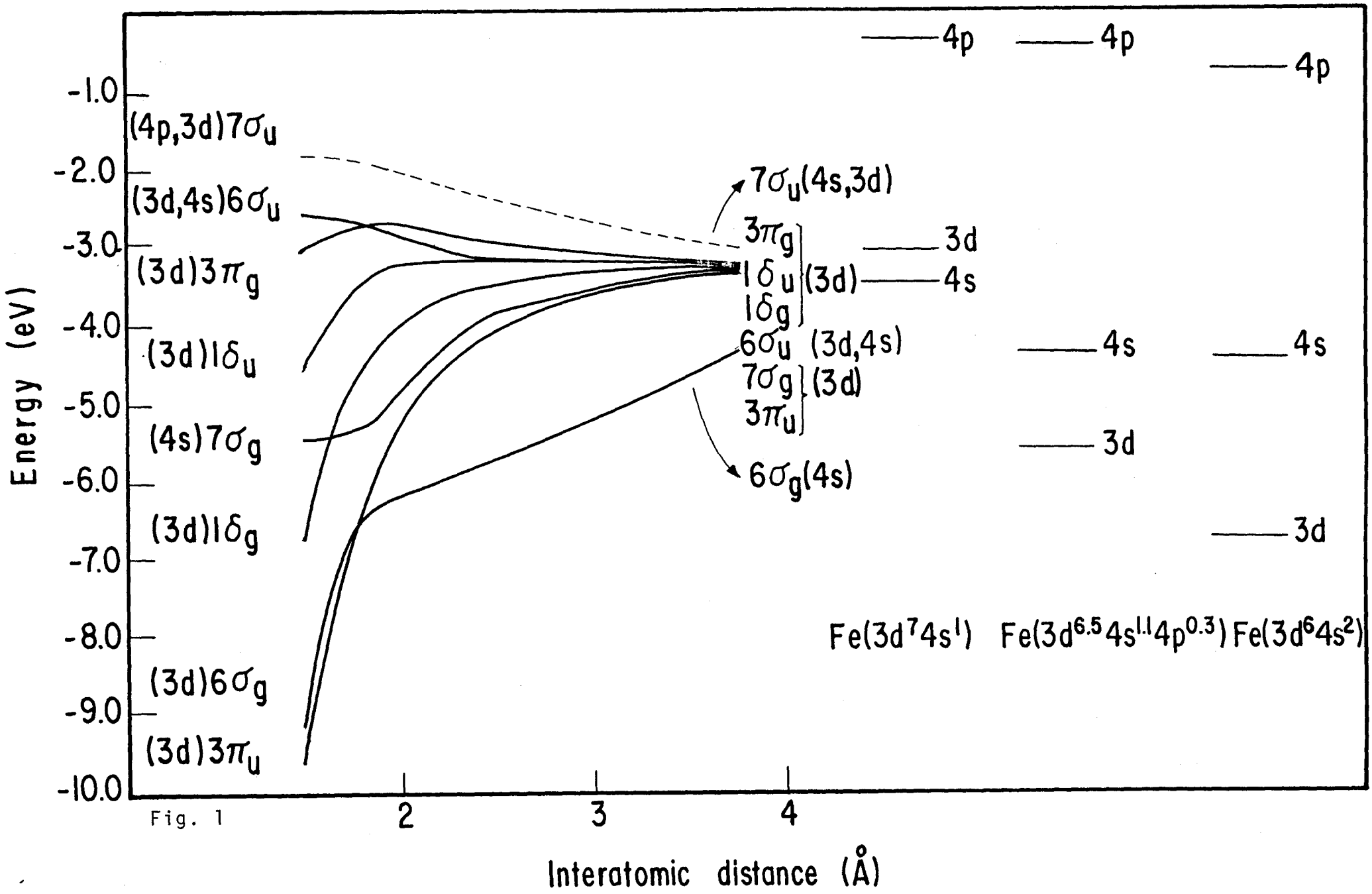
Energy (eV)
-1.0
-2.0
-3.0
-4.0
-5.0
-6.0
-7.0
-8.0
-9.0
-10.0
(4p,3d)7σu
(3d,4s)6σu
(3d)3πg
(3d)1δu
(4s)7σg
(3d)1δg
(3d)6σg
(3d)3πu
7σu(4s,3d)
3πg
1δu
1δg
(3d)
6σu (3d,4s)
7σg
3πu
(3d)
6σg(4s)
4p
4p
4p
3d
4s
4s
4s
3d
3d
Fe(3d74s1)
Fe(3d6.54s1.14p0.3)
Fe(3d64s2)
2
3
4
Interatomic distance (Å)

Fig. 1

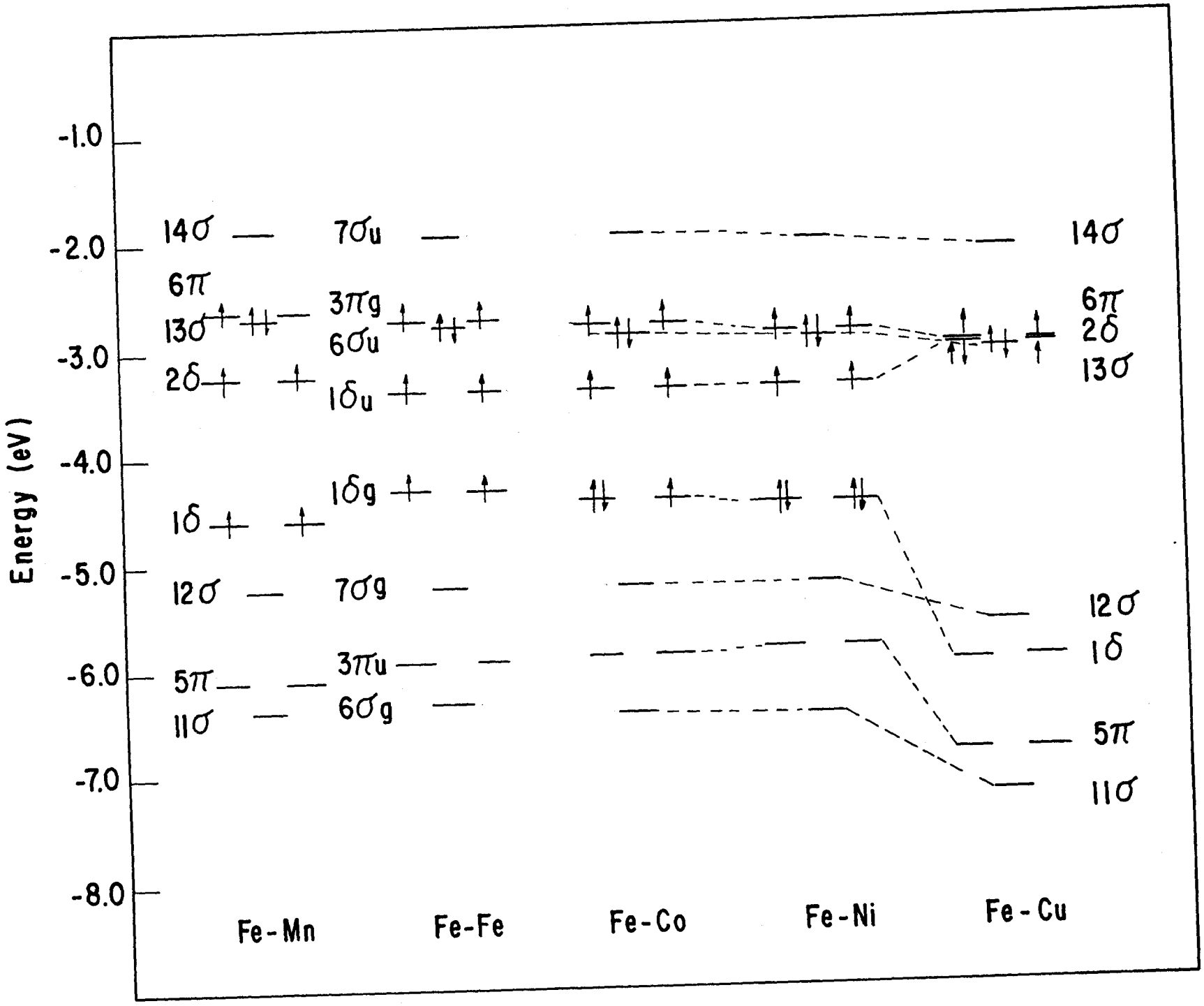
Energy (eV)
-1.0
-2.0
-3.0
-4.0
-5.0
-6.0
-7.0
-8.0
14σ
7σu
6π
3πg
13σ
6σu
2δ
1δu
1δg
1δ
12σ
7σg
5π
3πu
11σ
6σg
Fe-Mn
Fe-Fe
Fe-Co
Fe-Ni
Fe-Cu

Fig. 2

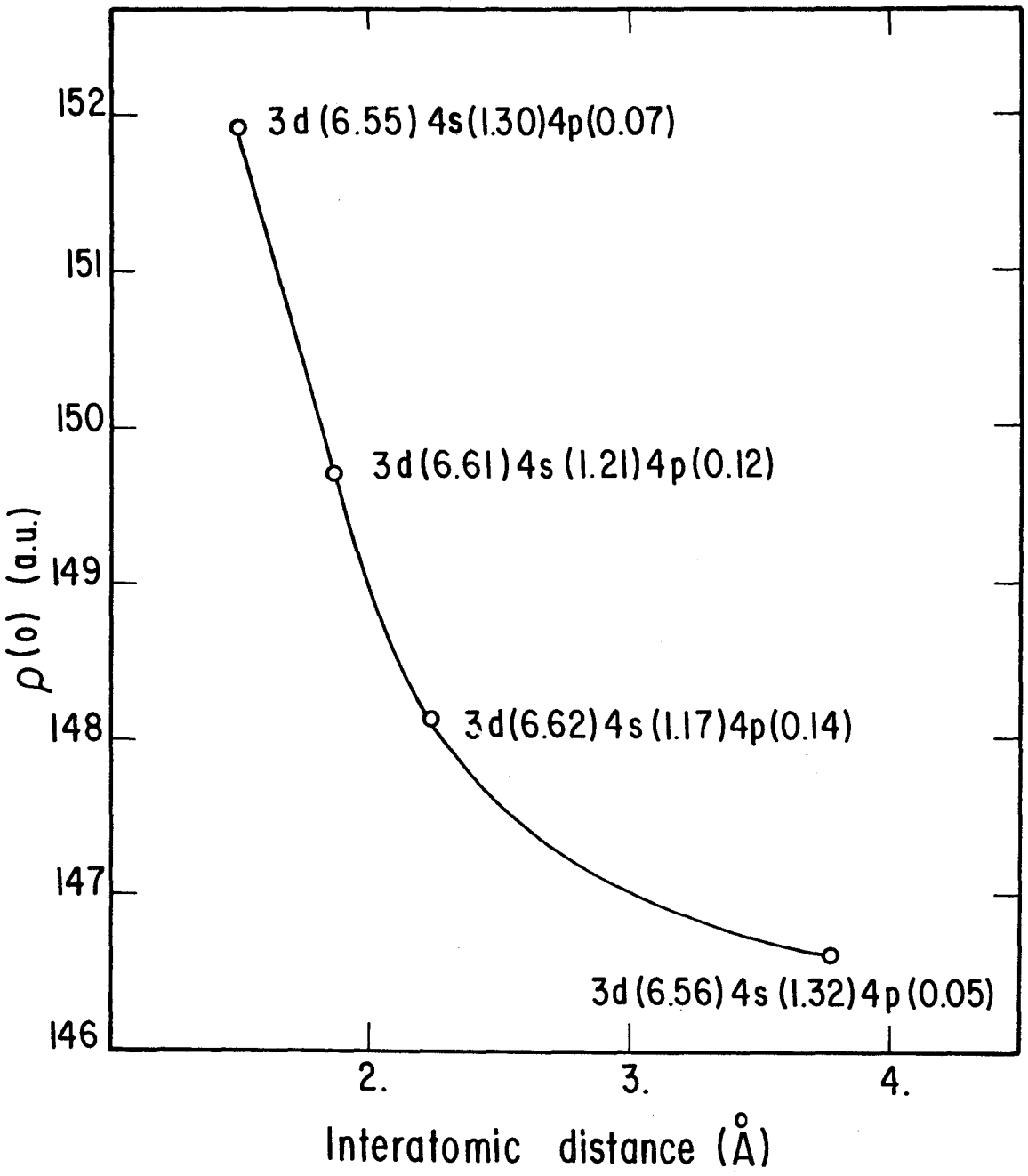
3d (6.55) 4s(1.30)4p(0.07)
3d(6.61)4s (1.21)4p(0.12)
3d(6.62)4s (1.17)4p(0.14)
3d (6.56) 4s (1.32)4p (0.05)
152
151
150
149
148
147
146
ρ(o) (a.u.)
2.
3.
4.
Interatomic distance (Å)

Fig. 3

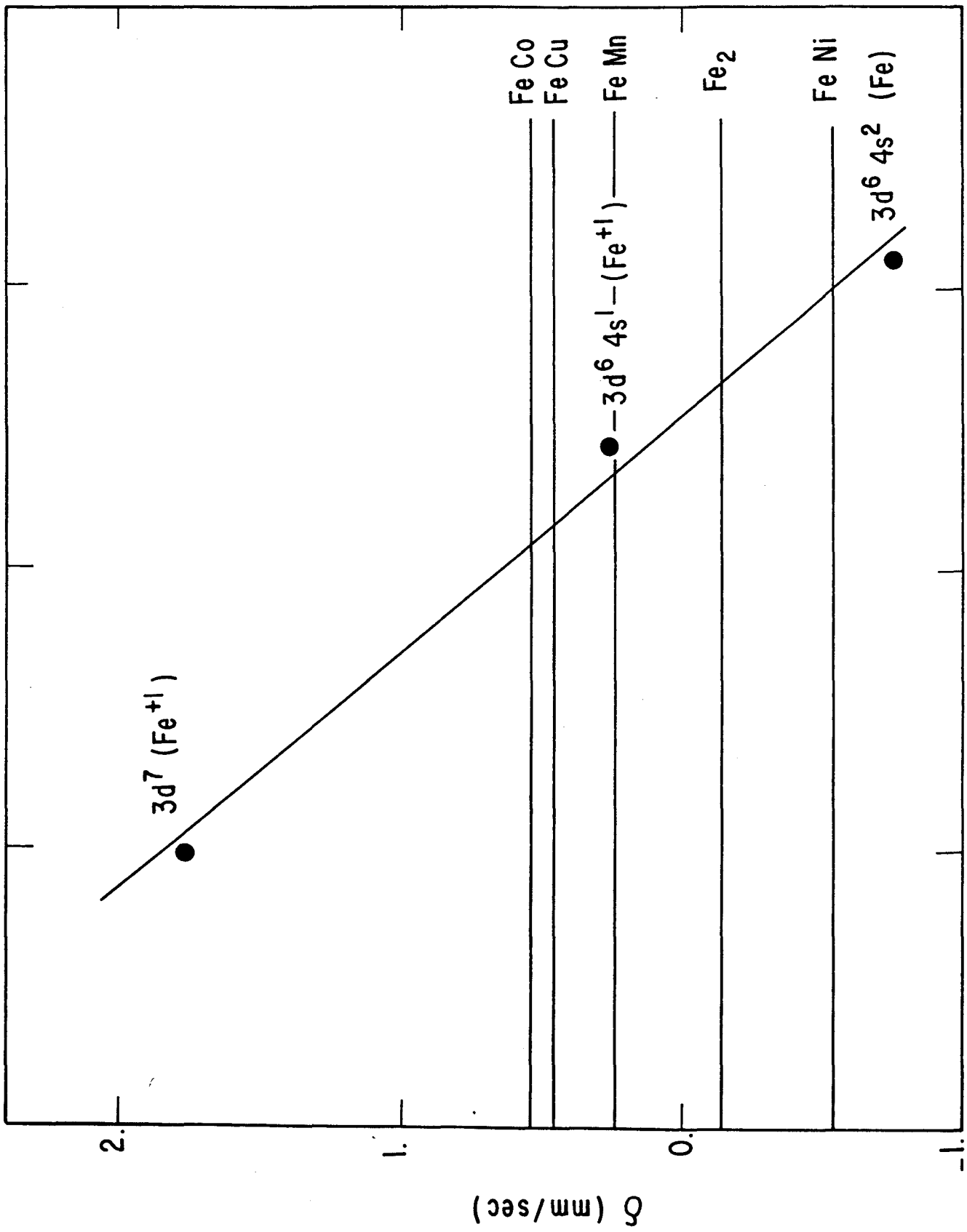
Fe Co
Fe Cu
Fe Mn
Fe2
Fe Ni
3d6 4s2 (Fe)
3d6 4s1 (Fe+1)
3d7 (Fe+1)
2.
1.
0.
-1.
δ (mm/sec)
135
140
145
150
ρ(0) (a0-3)

Fig. 4

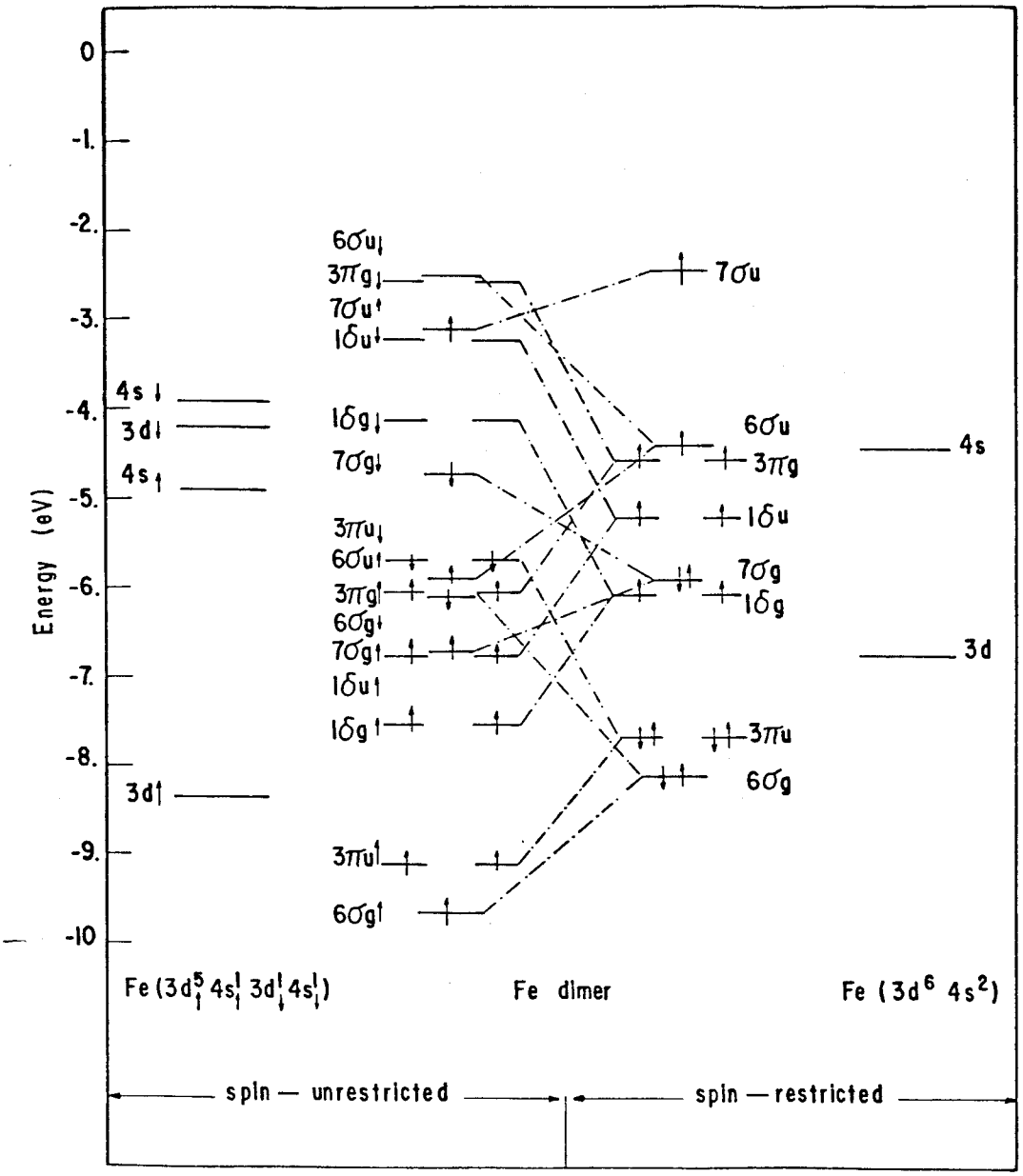
0
-1.
-2.
-3.
-4.
-5.
-6.
-7.
-8.
-9.
-10
Energy (eV)
4s↓
3d↓
4s↑
3d↑
6σu↓
3πg↓
7σu↑
1δu↓
1δg↓
7σg↓
3πu↓
6σu↑
3πg↑
6σg↓
7σg↑
1δu↑
1δg↑
3πu↑
6σg↑
7σu
6σu
3πg
1δu
7σg
1δg
3πu
6σg
4s
3d
Fe (3d↑5 4s↑ 3d↓ 4s↓)
Fe dimer
Fe (3d6 4s2)
spin — unrestricted
spin — restricted

Fig. 5

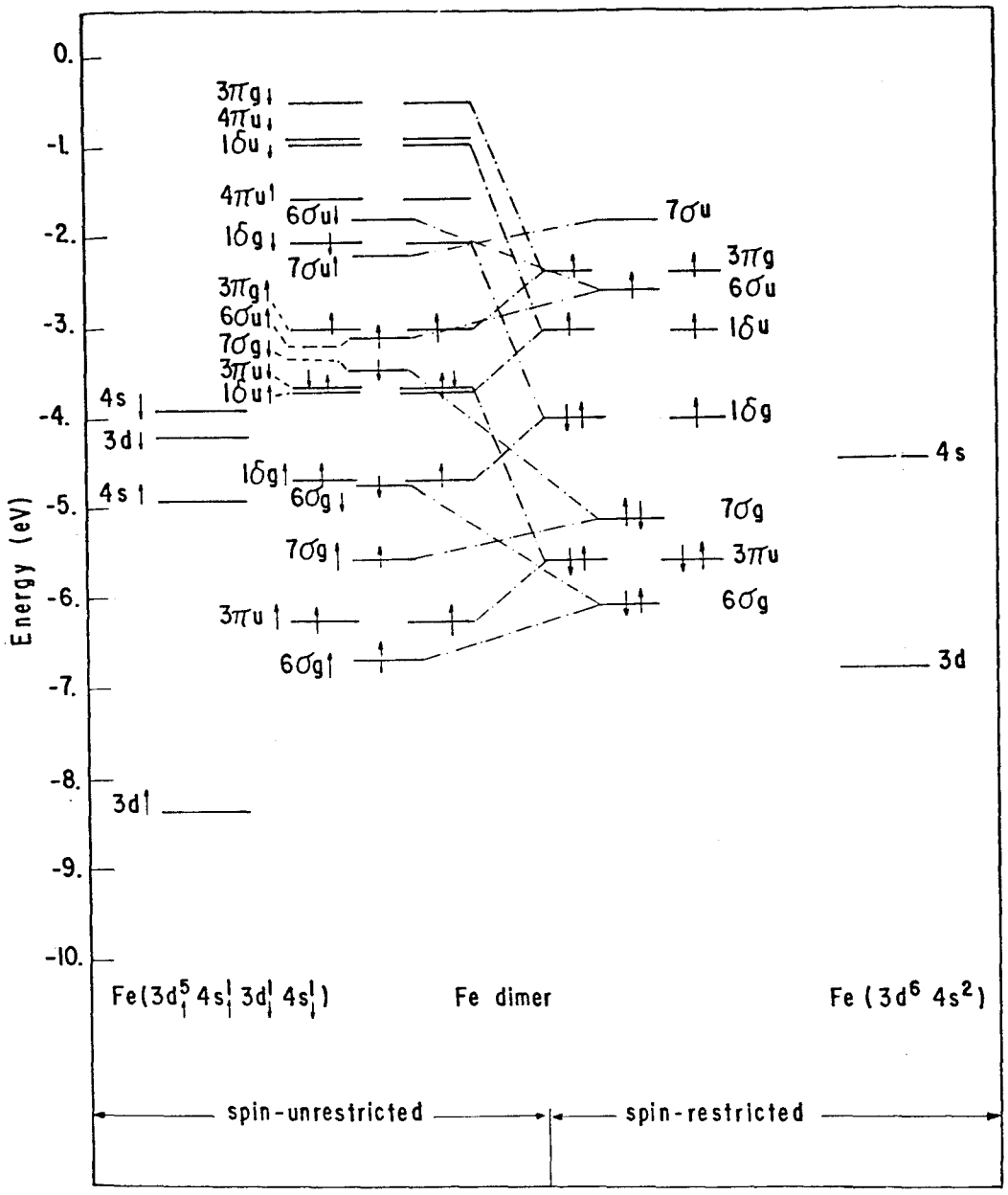
Energy (eV)
0.
-1.
-2.
-3.
-4.
-5.
-6.
-7.
-8.
-9.
-10.
3πg↓
4πu↓
1δu↓
4πu↑
6σu↓
1δg↓
7σu↓
3πg↑
6σu↑
7σg↓
3πu↓
1δu↑
4s↓
3d↓
1δg↑
6σg↓
4s↑
7σg↑
3πu↑
6σg↑
3d↑
7σu
3πg
6σu
1δu
1δg
7σg
3πu
6σg
4s
3d
Fe(3d↑5 4s↑ 3d↓ 4s↓)
Fe dimer
Fe (3d6 4s2)
spin-unrestricted
spin-restricted

Fig. 6

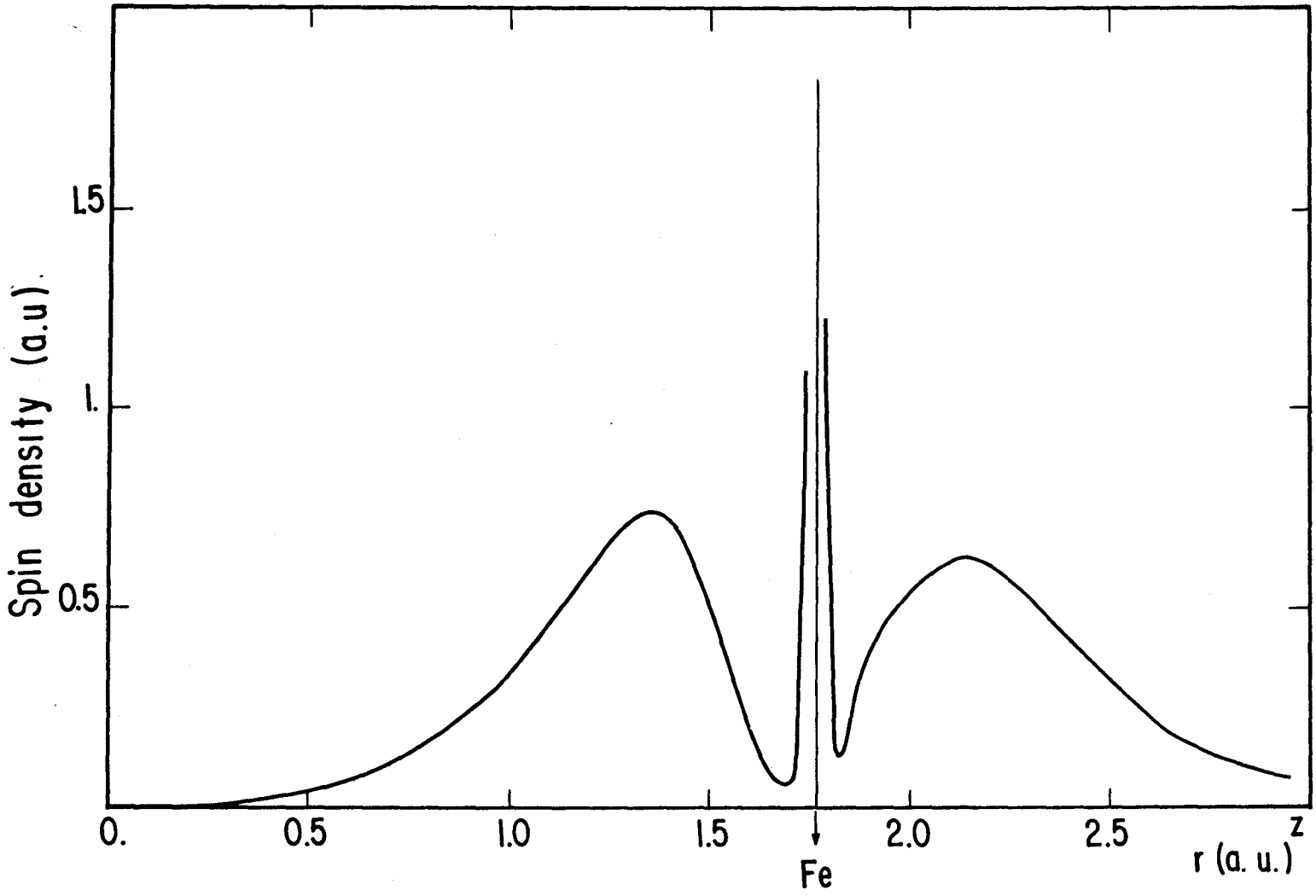

Fig. 7